Impact of the Control-Channel Transmission Rate in a Multi-Channel Wireless Network

Junseok Kim and Marwan Krunz
Department of Electrical and Computer Engineering
The University of Arizona, Tucson, AZ 85721
Email: {junseok, krunz}@ece.arizona.edu

***Abstract*—Multi-channel medium access control (MMAC) has the potential to significantly improve the network throughput by enabling parallel transmissions over different frequency channels. In many MMAC protocols, nodes exchange control packets over a dedicated control channel (CC). The CC transmission rate (CCR) is usually set to the lowest possible value, so as to maximize the reachability of control packets. However, in a multi-hop ad hoc network, this choice of the CCR may lead to a CC bottleneck, especially under high traffic load. While increasing the CCR can alleviate this bottleneck and improve the single-hop MMAC performance, it may also increase the number of hops along the path and hence degrade the end-to-end network performance. In this paper, we investigate the impact of the CCR on the performance of a multi-channel, multi-hop wireless network under a general MMAC protocol. To derive the queuing and channel access delays, we model the network as a G/G/1 queuing system. In our analysis, we consider detailed packet-level operations and non-saturated traffic. The average number of hops is also analytically obtained when nodes are randomly distributed. Our analysis is evaluated via network simulations, using 802.11a parameters. The simulation and numerical results reveal that the lowest transmission rate is not the optimal CCR. Our simulations show that the received power threshold has a significant impact on the optimal CCR.**

***Keywords*-Multi-channel system, control channel rate, MMAC, performance analysis**

I. Introduction

Thanks to advances in physical-layer technologies, wireless LAN interfaces have rapidly increased their speeds, reaching 54 Mbps for 802.11a/g devices and 600 Mbps for 802.11n devices [1]. These values represent the peak *link-layer* data rates. When accounting for MAC overheads (e.g., random backoff, control packets, etc.), the actual bandwidth available to applications is almost halved [2].

The throughput performance of wireless transmissions can be significantly improved by employing multiple frequency channels. Efficient utilization of such channels in a multi-user, networked environment necessitates employing a multi-channel MAC (MMAC) protocol. In MMAC protocols, senders and receivers exchange control packets over a control channel so as to select the best available data channel(s). The data packet is then transmitted over the selected data channel(s). The IEEE 802.11a/n standards, which operate in the 5 GHz ISM band, provide up to 23 non-overlapping channels [1]. Ideally, 23 data packets can be transmitted simultaneously in the same vicinity.

Under high traffic load, the control channel (CC) can get congested and becomes a performance bottleneck. Many papers have been presented to solve this problem [3][4][5][6][7]. CC hopping was applied in [3][4] to distribute the CC overload over various channels. In [5][6], nodes periodically have data channel negotiation phase over the CC to reduce collisions and improve channel utilization. Most of MMAC protocols generally take the CCR to be the lowest transmission rate supported by the network.

Intuitively, increasing the CCR can alleviate the CC bottleneck and improve the network performance in a single-hop network. However, this may not be true in a multi-hop network. In this paper, we investigate the impact of the CCR on the average end-to-end network performance, under a general MMAC protocol. To obtain the per-hop queuing and channel access delay, we model the CC access as a G/G/1 queuing system. In our analysis, we consider detailed packet-level operations and non-saturated traffic. A multi-channel extension of the 802.11 DCF approach with RTS/CTS handshake is used as an access scheme for the CC. We consider rate adaptation over the data channels, based on the distance between the sender and the receiver. The average number of hops is also analytically obtained when nodes are randomly distributed. NS-3 is used to evaluate our analysis, applied to 802.11a settings.

Our results show that the lowest transmission rate is not the optimal CCR that minimizes the end-to-end delay. We conduct extensive simulations to study the impact of different parameters on the optimal CCR. Our results show that the receive power threshold has a profound impact on the selection of optimal CCR. The optimal CCR can be as high as 18 Mbps, depending on the value of this threshold. To the best of our knowledge, this is the first study of the optimal CCR in a multi-channel multi-hop wireless network. Our analytical framework does not require a specific traffic generation model, routing protocol, or node distribution.

The remainder of the paper is organized as follows. Related works are discussed in Section II. We overview the general operation of MMAC protocols in Section III. In Section IV, we describe an analytic framework to model

978-1-4673-5828-6/13/ $31.00

a wireless multi-channel, multi-hop network. Section V and VI present numerical results and extensive simulations, respectively. Section VII concludes the paper.

II. Related Works

A. CC Bottleneck in Multi-Channel Systems

MMAC protocols have been extensively studied for wireless ad hoc networks, sensor networks [8], and more recently, cognitive radio networks [9]. These works are broadly categorized according to the time scale of channel assignment, into packet based, node based, and flow based. In this paper, we focus on the first category.

Using a dedicated CC for network coordination and parameter negotiation is a common practice in MMAC protocols. With this approach, control packets such as the *request-to-send* (RTS) and the *clear-to-send* (CTS) are exchanged over the CC and are used (among other purposes) to select the best available data channel(s). Under high traffic load, the CC can become a performance bottleneck and a single point of failure for the network. To alleviate this problem, the authors in [3][4] presented channel hopping algorithms. In [3], nodes hop according to a common channel hopping sequence (CHS). If a sender seizes the channel after a random backoff period, this sender and the corresponding receiver remain on the current channel until the data transmission is completed. In [4], each node has a unique CHS so that nodes have to know the CHSs of their neighbors. The channel-hopping-based approach requires stringent time/channel synchronization between nodes.

In [7], the frequency bandwidth of the CC is adjusted according to the traffic load. This solution is not achievable in IEEE 802.11-based networks because channels in the 802.11 scheme have the same bandwidth. In [11], source nodes use a heuristic approach to adjust the packet generation rate according to the degree of congestion on the CC. If the number of messages in the MAC queue exceeds a predefined threshold, the source node reduces the packet generation rate. If it is below another predefined threshold, the source node increases its packet generation rate. In between the two thresholds, the rate remains the same.

B. MMAC Performance Analysis

The single-hop performance of an MMAC was analytically investigated in [12] under saturated traffic and in [13] under non-saturated traffic. The end-to-end performance of an MMAC was analyzed in [14][15] for multi-hop networks. These works assume that the average number of hops is given. In [14], an *M/M/1/m* queuing system was used to obtain the delay for m data channels, but the overhead of the MAC layer (including random backoff and collisions) was not considered. An M/G/1 queuing system was used in [15] to carry out similar analysis but while taking into account the MAC operation. However, an oversimplified (slotted Aloha) access scheme was assumed for the CC. To analyze the non-saturated traffic case, packet arrivals were modeled as a Poisson process in [13][14][15]. In [16], upper and lower bounds on the network capacity were derived for a multi-channel, multi-hop network without considering the MAC-layer overhead. All of above works assumed that all data channels have the same capacity.

The work of D. Malone et. al. [17] modeled the 802.11 CSMA/CA in a non-saturated case but in a single collision domain.

III. Multi-channel MAC Protocol

Many MMAC protocols have been proposed in the literature. In this section, we illustrate the basic operation of an MMAC protocol, with a common CC. Then, in the next section, we analyze the MMAC performance by considering this operation.

Before transmitting a data packet over a data channel (DC), a sender and receiver exchange control packets over the CC. This exchange is an extension of the two-way RTS/CTS handshaking scheme used in the IEEE 802.11 standard. A sender performs a random backoff before transmission. If at least one DC is available and the CC is idle for the DCF interframe spacing (DIFS), the sender starts decrementing its backoff counter. The backoff counter is decreased by 1 if the CC is sensed idle in a backoff slot. If the CC is sensed busy, the sender freezes its backoff counter.

Once the backoff counter reaches zero, the sender transmits an RTS packet, containing the sender's available data channel list (channels for which the NAV values are zero). Upon receiving the RTS, the receiver selects one of commonly available DC and replies with a CTS packet. Different criteria can be used for DC selection, including channel quality and link capacity. In addition to specifying the DC to be used, the CTS can also include the transmission power and transmission rate for the DC. Upon receiving the CTS, the sender transmits a *decide-to-send* (DTS) packet, announcing the DC that will be used and the duration of this usage. This DTS is needed to inform the neighbors of the sender about the DC that will be reserved for the upcoming transmission. After transmitting the DTS, the sender begins data transmission over the DC. Upon receiving the data packet, the receiver replies with an ACK packet.

Once the DTS transmission is completed, the CC becomes available for other data transmissions. As the traffic load increases, the CC becomes a performance bottleneck, resulting in underutilizing the DCs. Because control packets are often transmitted using the lowest possible transmission rate, rate adaption over the DCs can worsen the CC bottleneck. Intuitively, increasing the CCR can alleviate this bottleneck in a single-hop network. However, in a multi-hop network, increasing the CCR can degrade the end-to-end performance because it increases the number of hops. In the next section, we analyze the end-to-end MMAC performance *with respect to the CCR*.

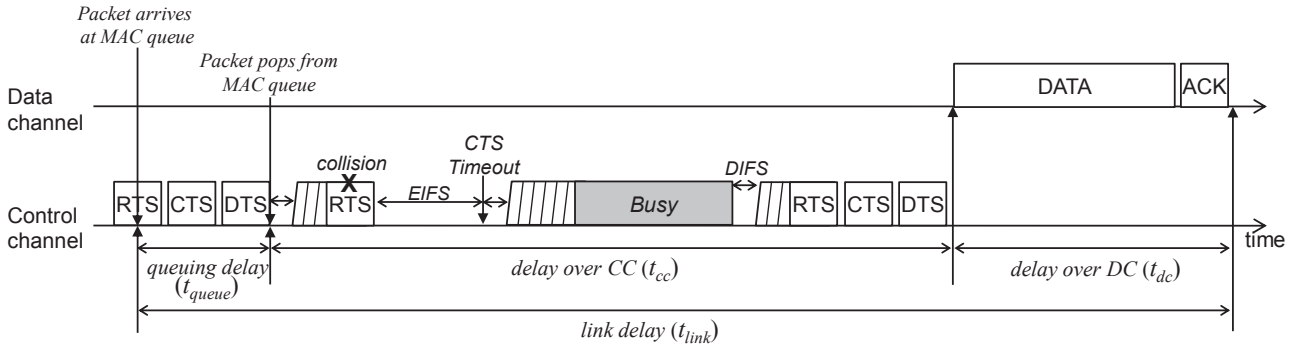

Figure 1. Timing diagram of channel access in a generic MMAC.

Table I
SUMMARY OF NOTATION.

Notation	Description	Notation	Description	Notation	Description
N	Number of nodes	a	Square length	k	Number of channels
l_{rts}	RTS packet size	l_{cts}	CTS packet size	l_{dts}	DTS packet length
l_{data}	DATA packet size	l_{ack}	ACK packet size	t_{sifs}	SIFS period
l_{difs}	DIFS period	t_{slot}	Slot duration	t_{pre}	Preamble duration
d_0	Close-in distance	η	Path loss exponent	P	Transmission power
P_{cs}	Carrier sense threshold	m	Number of backoff stages	w	RTS retransmission limit
h	Number of hops	λ	Packet generation rate	q	Routing probability
t_{queue}	Delay in MAC queue	t_{cc}	Channel access delay	t_{dc}	Data transmission delay
t_{link}	Link delay	Γ	Set of transmission rate	γ_i	ith transmission rate
s	Service time	e	Visit ratio	ρ	Traffic intensity
p	Collision probability	l	Source-destination distance	z	Transmitter-receiver distance
P_0	Path loss at d_0	γ_{ccr}	Transmission rate for CC	γ_{dcr}	Transmission rate for DC
Notation	Description				
q_{ji}	Routing probability that a packet is forwarded from node j to node i				
$\lambda_{ji}(\lambda_i)$	Packet arrival rate from node j to node i (Overall packet arrival rate at node i)				
$\xi_i(r_i)$	Received power threshold (maximum transmission range) that corresponds to γ_i				
$W_{min(max)}$	Minimum (maximum) contention window				
$c_a^2(c_s^2)$	Squared coefficient of variation for arrival (service) time				
τ	Probability that a node transmits in a randomly chosen backoff slot				
$\tilde{n}(\hat{n})$	Average number of neighbors within carrier sensing range (transmission range defined by CCR)				
p_{idle}	Probability that CC is idle in a given slot				
$p_{succ(coll)}$	Probability that successful transmission (collision) occurs in a given slot				

IV. Performance Analysis

A. Problem Setup

We consider an ad hoc network of N nodes. Nodes are randomly distributed over an $a \times a$ square. Each node operates as a source node, with a randomly chosen destination. The inter-packet generation times at each source node form an i.i.d random process with a mean rate λ. The size of a data packet including all headers is denoted by l_{data}. If a source node does not have a direct link to a destination, a multi-hop path is established based on the greedy forwarding scheme [18]. In this scheme, a sender forwards a data packet to the neighbor closest to the destination.

Packets generated at a source node are added to the tail of the MAC queue at that node. We assume that the queue size is sufficiently large. When a data packet is taken out of the MAC queue, a new random backoff value is generated from the interval [0, $CW-1$], where *CW* is the contention window size. Let W_{min} and W_{max} denote the minimum and maximum values for *CW*. Upon detecting a collision, a sender doubles its *CW* and restarts the backoff process.

Let $m = \log_2(W_{max}/W_{min})$ denote the number of backoff stages. Table I depicts the main notation used in our analysis.

We assume that there are k frequency channels that have the same Fourier bandwidth. One channel is designated as the CC and the remaining $k-1$ channels are used for data. We assume that a node can transmit and/or receive signals over multiple channels using the orthogonal frequency division multiple access (OFDMA) technique. More specifically, we assume half-duplex operation over the same channel but full-duplex operation over different channels. Its feasibility is proved in hardware in [19].

Let $\Gamma = \{\gamma_1, \gamma_2, ..., \gamma_i\}$ be the set of supported transmission rates. Let ξ_i be the received power threshold that corresponds to γ_i. The transmission power is fixed at P. Let r_i be the maximum transmission range associated with γ_i. This r_i is specified based on the log-distance path loss model, as follows [20]:

$$r_i = d_0 10^{\frac{P-\xi_i-P_0}{10\eta}} \tag{1}$$

where d_0, P_0, and η are the close-in reference distance, the path loss at d_0, and the path loss exponent, respectively. We assume the protocol model in our analysis. That is, a receiver cannot decode a packet if there are more than one transmission within its neighborhood.

All nodes have the same CCRs denoted by γ_{ccr}, where $\gamma_{ccr} \in \Gamma$. Let $\gamma_{dcr} \in \Gamma$ denote the transmission rate for the DC. It is selected by the receiver using (1) as in [21].

B. Average End-to-End Delay Analysis

Because nodes are randomly distributed, and the source and destination pairs are also randomly chosen, we assume that the traffic intensity at each node is, on average, the same. So the mean link access delay, denoted by $E[t_{link}]$, is the same for every link. For certain topologies (e.g., sphere or torus), this assumption is valid. For a square or circle, this is an approximation.

Let h denote the number of hops between a source and a destination. Then, the average end-to-end delay is $E[t_{e2e}] = E[t_{link}h] = E[t_{link}]E[h]$. The link delay is divided into three components: delay in the MAC queue, denoted by t_{queue}, random backoff and control packet exchange delay over the CC, denoted by t_{cc}, and data transmission delay over the DC, denoted by t_{dc}.

To derive t_{queue} and t_{cc}, we model the network as an open queuing network, as in [22][23]. Specifically, each node is modeled as a G/G/1 system. Customers are requests for data transmission generated by the node itself or routed from other nodes. Because of our assumption of full-duplex capability over different channels, nodes can contend over the CC while transmitting or receiving over the DCs. The service time, denoted by s, is the duration from when a packet is taken from the HOL of the MAC queue until it is about to be transmitted over the DC (after contention and control packet exchanges). Note that $s = t_{cc}$.

Let λ_{ji} denote the packet arrival rate from node j to node i. Let λ_{0i} denote the intrinsic packet arrival rate of node i. In our problem setup, $\lambda_{0i} = \lambda$ for all i. The overall packet arrival rate at node i is given by:

$$\lambda_i = \lambda_{0i} + \sum_{j=1, j\neq i}^{N} \lambda_j q_{ji} \tag{2}$$

where q_{ji} is the routing probability that a packet is forwarded from node j to node i. Let e_i be the mean number of visits of a packet to node i (a.k.a. *visit ratio*), given by:

$$e_i = \frac{\lambda_i}{\sum_{i=0}^{N} \lambda_{0i}}. \tag{3}$$

Let $c_{a_i}^2$ and $c_{s_i}^2$ denote the squared coefficient of variation for the arrival and service times at node i, respectively. c_{a_i} and c_{s_i} have the following relationship [22]:

$$c_{a_i}^2 = 1 + \sum_{j=1, i\neq j}^{N} \left(c_{s_j}^2 - 1\right) (q_{ji})^2 e_j e_i^{-1}. \tag{4}$$

Our primary goal is to find the optimal CCR that minimizes the average end-to-end delay. Because nodes have the same average performance, we drop the index i from our notation. Similarly, q_{ji} is simplified as follows [23]:

$$q_{ji} = \frac{q}{N-1} = \frac{1 - \frac{1}{E[h]}}{N-1}, \forall i, j, i \neq j \tag{5}$$

where q is the routing probability that a packet is forwarded to another node. Then, c_a^2 reduces to:

$$c_a^2 = 1 + (c_s^2 - 1)\left(1 - \frac{1}{E[h]}\right). \tag{6}$$

If c_s^2 is given, the mean waiting time in the service station is obtained as follows [22]:

$$E[t_{queue}] + E[s] \quad = \quad \frac{\rho}{1 - \exp\left\{-\frac{2(1-\rho)}{c_a^2\rho + c_s^2}\right\}} \tag{7}$$

where ρ denotes the traffic intensity (a.k.a. server utilization).

Because all source nodes generate packets with the mean rate λ, the overall traffic load at a node (including intrinsic plus relayed traffic) is $\lambda E[h]$ (the total traffic in the network is, on average, $\lambda N E[h]$). Then, the traffic intensity is given by $\rho = \lambda E[h] \cdot E[s]$.

During each time slot of the random backoff process, the channel state at a node will be in one of three possible states: idle channel (E_{idle}), successful transmission (E_{succ}), and collision (E_{coll}). Let $p_{idle} = P\{E_{idle}\}$, $p_{succ} = P\{E_{succ}\}$, and $p_{coll} = P\{E_{coll}\}$ denote the corresponding probabilities. The mean service time is given by [24]:

$$E[s] \quad = \quad \frac{\alpha\left(W_{min}\beta - 1\right)}{2\left(1-p\right)} + \frac{p}{(1-p)} t_{coll} \tag{8}$$

where

$$\alpha = t_{slot}p_{idle} + t_{succ}p_{succ} + t_{coll}p_{coll} \quad (9)$$

$$\beta = \frac{1-p-2^m p^{(m+1)}}{1-2p} \quad (10)$$

In the above equations, p is the collision probability when the tagged node transmits an RTS, t_{slot} is the backoff slot time, and t_{succ} (t_{coll}) is the time the CC is sensed busy due to a successful transmission (collision), respectively.

Following [17], we assume that t_{succ} and t_{coll} are same, and are given by:

$$t_{succ} = t_{coll} = \frac{(l_{rts}+l_{cts}+l_{dts})8}{\gamma_{ccr}} + t_{difs} + 2t_{sifs} + 3t_{pre} \quad (11)$$

where l_{rts}, l_{cts}, and l_{dts} are the sizes of the RTS, CTS, and DTS packets, respectively; and t_{difs}, t_{sifs}, and t_{pre} are the DIFS, the short interframe spacing (SIFS), and the preamble duration, respectively.

The three probabilities in (9) are given by [24]:

$$p_{idle} = (1-\tau)^{\tilde{n}-1} \quad (12)$$

$$p_{succ} = (\tilde{n}-1)\tau(1-\tau)^{\tilde{n}-2} \quad (13)$$

$$p_{coll} = (1-p_{idle})\left(1 - \frac{p_{succ}}{1-(1-\tau)^{\tilde{n}-1}}\right). \quad (14)$$

where τ is the probability that a node transmits in a randomly chosen backoff slot and $\tilde{n} = N(\pi\tilde{r}/a^2)$ is the average number of neighbors within the carrier sensing range $\tilde{r}$.

To compute c_s^2, we need to determine the variance of the service time (σ_s^2). This quantity is given by [24]:

$$\sigma_s^2 = \left[\frac{\alpha\,(W_{min}\delta - 1)}{2} + t_{coll}\right]^2 \frac{p}{(1-p)^2} \quad (15)$$

where

$$\delta = \frac{\left[2p^2 - 1 - m(1-2p)(1-p)\right]\left[2p^m + 2(1-p)^2\right]}{(1-2p)^2}. \quad (16)$$

For an unsaturated network, p in (15) is defined as follows [17]:

$$p = 1-(1-\tau)^{\overline{n}-1} \quad (17)$$

where

$$\tau = b\left(\frac{\rho^2 W_{min}}{(1-p)(1-\rho)(1-(1-\rho)^{W_{min}})} - \frac{\rho^2(1-p)}{1-\rho}\right) \quad (18)$$

and

$$\frac{1}{b} = (1-\rho) + \frac{\rho^2 W_{min}(W_{min}+1)}{2(1-(1-\rho)^{W_{min}})} + \frac{\rho(W_0+1)}{2(1-\rho)} \cdot \left[\frac{\rho^2 W_{min}}{1-(1-\rho)^{W_{min}}} + (1-(1-\rho))(1-\rho) - \rho(1-p)(1-p)\right] + \frac{p\rho^2}{2(1-\rho)(1-p)} \cdot \left[\frac{W_0}{1-(1-\rho)^{W_{min}}} - (1-p)(1-p)\right] \cdot \left[2W_{min}\frac{1-p-p(2p)^{m-1}}{1-2p} + 1\right] \quad (19)$$

Let r_{ccr} denote the transmission range that corresponds to γ_{ccr}. In (17), $\overline{n} = N \cdot (\pi r_{ccr}^2/a^2)$ is the average number of neighbors within the transmission range defined by the CCR. Using (15), and (17), we can compute σ_s^2.

The average value of t_{dc} is derived as follows:

$$E[t_{dc}] = \frac{(E[l_{data}] + l_{ack}) \cdot 8}{E[\gamma_{dcr}]} + t_{sifs} \quad (20)$$

where l_{ack} is the size of the ACK packet and $E[\gamma_{dcr}]$ is the mean transmission rate for a DC. This $E[\gamma_{dcr}]$ is obtained as follows:

$$E[\gamma_{dcr}] = \int_0^r g(z) \cdot f_{\mathbf{z}}(z)\,\mathrm{d}z \quad (21)$$

where $g(\cdot)$ is a function that conveys the relationship between the transmitter-receiver distance, denoted by z, and the maximum possible transmission rate at that distance. (Typically, $g(\cdot)$ takes the shape of a staircase.) $E[h]$ is obtained as follows [18]:

$$E[h] = \int_0^r \int_0^{\sqrt{2}a} \lceil l/z \rceil f_{\mathbf{l}}(l) f_{\mathbf{z}}(z)\,\mathrm{d}l\mathrm{d}z. \quad (22)$$

In (21) and (22), $f_{\mathbf{z}}(z)$ is the probability density function (PDF) of z. For the greedy routing protocol, $f_{\mathbf{z}}$ is given by [18]:

$$f_{\mathbf{z}}(z) = \begin{cases} \Sigma_{i=0}^{\infty} \frac{\zeta^i}{i!} e^{-\zeta} 2i \left(\frac{2}{\pi r_{ccr}^2}\right)^i (1-z) \cdot \\ \arccos\left(1 + \frac{z^2 - r_{ccr}^2}{2l(1-z)}\right) \cdot \\ \left[\frac{1}{2}\sqrt{4r^2l^2 - (r_{ccr}^2 - z^2 + 2lz)^2} - \right. \\ (l-z)^2 \arccos\left(1 + \frac{z^2 - r_{ccr}^2}{2l(l-z)}\right) + \\ \left. r_{ccr}^2 \arcsin\left(\frac{r_{ccr}^2 - z^2 + 2lz}{2lr_{ccr}}\right)\right]^{i-1} & 0 \le z \le r_{ccr} \\ 0 & \text{elsewhere} \end{cases}$$

where

$$\zeta = \frac{N\pi}{2}\left(\frac{r_{ccr}}{a}\right)^2 \quad (23)$$

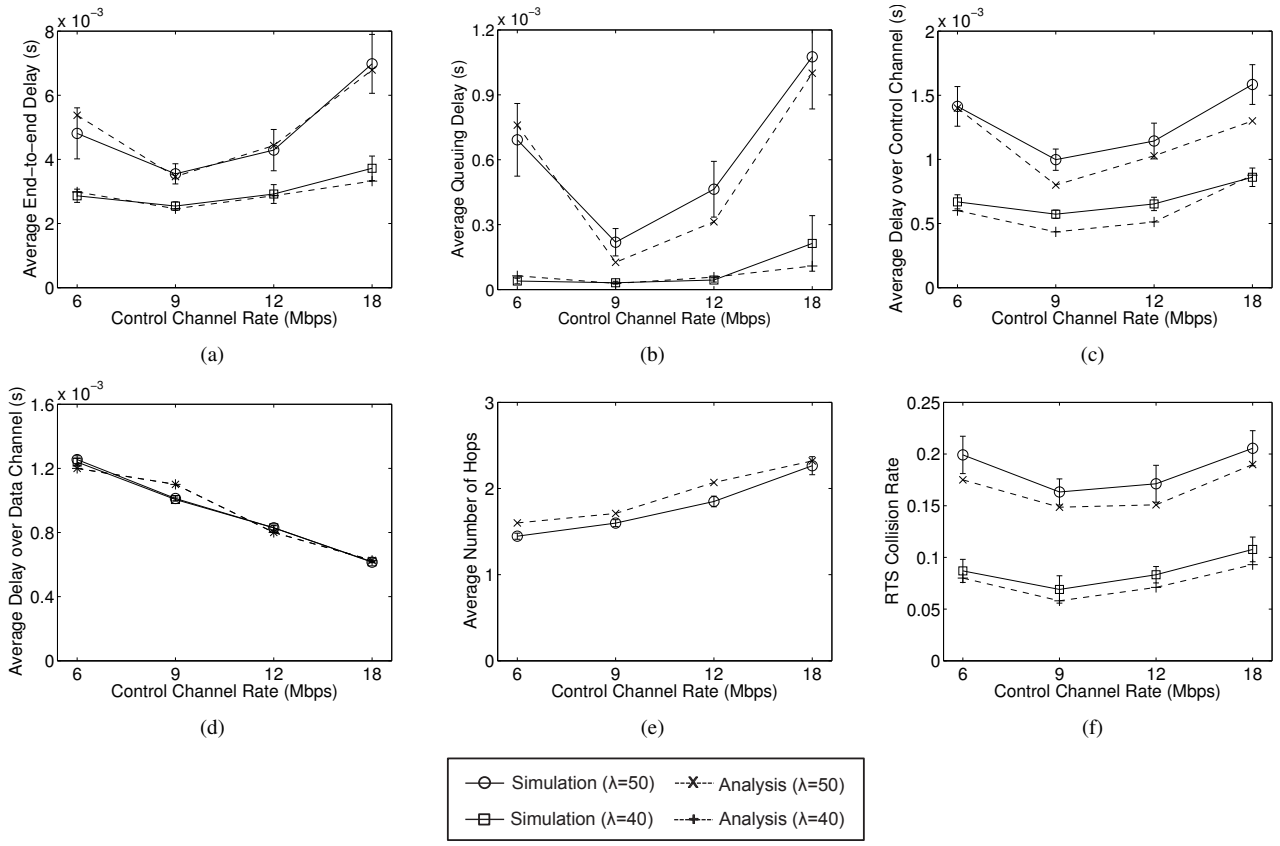

Figure 2. Comparison between analytical and simulation results.

and l is the direct distance between the source and final destination nodes. In the above analysis, we can use any other routing protocol with a given $f_{\mathbf{z}}(z)$. Recall that nodes are randomly distributed over an $a \times a$ square. For a square region, the PDF of l is given by [25]:

$$f_{\mathbf{l}}(l) = \begin{cases} \frac{4l}{a^4}\left(\frac{\pi}{2}a^2 - 2al + \frac{1}{2}l^2\right) & 0 \le l \le a \\ \frac{4l}{a^4}\left(a^2 \arcsin(\frac{a}{l}) + 2a\sqrt{l^2 - a^2}\right. & \\ \left. -a^2 - a^2 \arccos(\frac{a}{l}) - \frac{1}{2}l^2\right) & a \le l \le \sqrt{2}a \\ 0 & \text{elsewhere.} \end{cases} \tag{24}$$

We can apply the same approach to other shapes if their $f_{\mathbf{l}}(l)$ is known.

Finally, the average end-to-end delay is obtained using (7) and (20) as follows:

$$E[t_{e2e}] = E[t_{link}] \cdot E[h] = (E[t_{queue}] + E[t_{cc}] + E[t_{dc}])E[h]. \tag{25}$$

The final result is not in closed form and has to be obtained numerically. However, we can have some intuitions from equations. As the CCR increases, the duration of control exchanges reduces but the collision rate increases as in (11) and (17), respectively. It is not trivial to understand the impact of CCR on the duration of data/ACK exchanges and the number of hops from (20)-(23). However, intuitively $\gamma_{dcr} \ge \gamma_{ccr}$ and hence the duration of data/ACK exchanges decreases as the CCR increases. As the CCR increases, the maximum transmission range decreases and hence the number of hops increases.

Although we use some of existing models, the novelty of our work is extending these models to analyze the impact of CCR on the MMAC performance in wireless ad-hoc networks. Our analytical framework does not require a specific traffic generation model, routing protocol, and node distribution. It is also applicable to other channel access scheme if the first and second moments of the channel access delay are known. For example, we can analyze the performance of MMAC with contention-tree algorithm using the first and seconds moments provided in [26].

V. Validation of Analytical Results

To validate our analysis, we compared the analysis-based numerical results to NS-3 simulations. For this paper, we completely reprogram the MAC/PHY components for NS-3. The simulation scenario is similar to the one in Section IV-A, where 50 nodes are randomly distributed over 250 $\times$ 250 meter square. Each node operates as a source node with a randomly chosen destination. The greedy forwarding

Table II
SIMULATION PARAMETER VALUES [1].

Parameter	Value	Parameter	Value
N	50	a	250
l_{rts}	21 byte	l_{cts}	20 byte
l_{dts}	20 byte	l_{data}	1500 byte
l_{ack}	15 byte	t_{sifs}	16 us
l_{difs}	34 us	t_{slot}	9 us
t_{pre}	16 us	W_{min}	16
W_{max}	1024	d_0	1 m
η	2.7	P	23 dBm
P_{cs}	-110 dBm	k	11
m	7	w	6

Table III
TRANSMISSION RATES AND RECEIVE POWER THRESHOLDS FROM THE 802.11A STANDARD [1].

CCR ID	Modulation	FEC	TX Rate	Receive Power Threshold
8	QAM64	3/4	54 Mbps	-65.0 dBm
7	QAM64	2/3	48 Mbps	-66.0 dBm
6	QAM16	3/4	36 Mbps	-70.0 dBm
5	QAM16	1/2	24 Mbps	-74.0 dBm
4	QPSK	3/4	18 Mbps	-77.0 dBm
3	QPSK	1/2	12 Mbps	-79.0 dBm
2	BPSK	3/4	9 Mbps	-81.0 dBm
1	BPSK	1/2	6 Mbps	-84.0 dBm

protocol is used to establish multi-hop routes. Each source node generates 1500 byte UDP packets according to a Poisson process with a given mean rate. Other simulation parameters are based on the IEEE 802.11 standard, and are listed in Tables II and III.

Figure 2 shows the average performance for the two mean packet generation rates. Hereafter, error bars represent 95% confidence intervals. The figure shows that 9 Mbps (not 6 Mbps) is the optimal CCR, regardless of the packet generate rate. The average queuing delay ($E[t_{queue}]$), the average delay over CC ($E[t_{cc}]$), and the RTS collision rate (p) also reflect the optimality of the CCR at 9 Mbps. When the CCR increases from 6 to 9 Mbps, the duration of control packet exchange (t_{succ}) is reduced by 14.5% and the number of hops is increased by 10.5%. In this case, the transmission time of control packets and the number of nodes in a collision domain are reduced. Hence, the delay and the collision rate are decreased.

When the CCR increases from 9 to 12 Mbps, the duration of control packet exchange is reduced by 8.5% and the number of hops is increased by 15.69%. In this case, the increase in the number of hops plays a more critical role in the average performance than the decrease in the minimum CC overhead. Because DIFS, SIFS, and the preamble duration are fixed regardless of the CCR, the reduction in the CC overhead slows down as the CCR increases. In addition, the higher the number of hops, the more transmissions are required to deliver messages to their destinations. As a consequence, the traffic intensity and the collision probability increase when the CCR increases beyond 9 Mbps. The average delay over DCs ($E[t_{DC}]$) monotonically decreases as the CCR decreases. However, the reduction in $E[t_{DC}]$ does not much impact the average end-to-end delay.

There are some discrepancies between the analysis and the simulations in the average queuing delay and the average delay over the CC. This is related to ignoring the effect of hidden terminals in the analysis of the collision probability.

VI. SIMULATION RESULTS

Next, we conduct extensive simulations to understand the impact of various factors on the optimal CCR. We vary the data size, the path loss exponent, and the received power threshold, respectively. Unless stated otherwise, other parameters are the same as in Table II.

Figure 3 depicts the average performance versus the CCR for two different data packet sizes. Regardless of the packet size, the optimal CCR is 9 Mbps. The average queuing delay is not affected by the packet size. Because data packets are transmitted over DCs, the average delay over the CC is not affected by data size. The difference in the average end-to-end delay results between the simulation and and analysis is due to the difference in the average delay over the DCs. These differences narrows down as the CCR increases, because SIFS (between data and ACK) and preamble durations are fixed, regardless of the CCR.

Figure 4 shows the average performance versus the CCR for two different path loss exponents. Regardless of the value of η, the optimal CCR is 9 Mbps. The higher path loss exponent, the more gradual the reduction in the transmission range. When $\eta = 2.7$, the transmission ranges are 143, 130, and 110 meters for 6, 9, and 12 Mbps, respectively. When $\eta = 3$, the transmission ranges are 86, 80, and 69 meters for 6, 9, and 12 Mbps, respectively. The differences between transmission ranges are smaller when $\eta = 3$ than when $\eta = 2.7$. However, the increase in hop count is slightly more steeper when $\eta = 3$ than when $\eta = 2.7$, as shown in Fig. 4(c). Denote the forward progress from the sender to a relay node, relative to the transmission range by z. When the node density is same, z increases as the path loss exponent increases, so that the impact of the number of hops also grows.

Figure 5 shows the average performance versus the CCR using the transmission rate/received power threshold table of the Cisco Aironet 1250 chipset. We replace the received power thresholds in Table III with the ones used in [27].

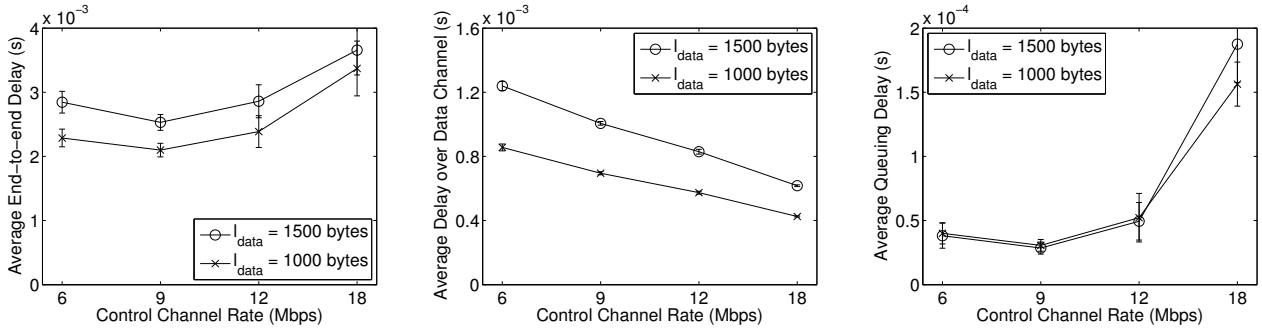

Figure 3. Average performance versus the CCR for different data packet sizes: ($\lambda = 40$ packets/sec).

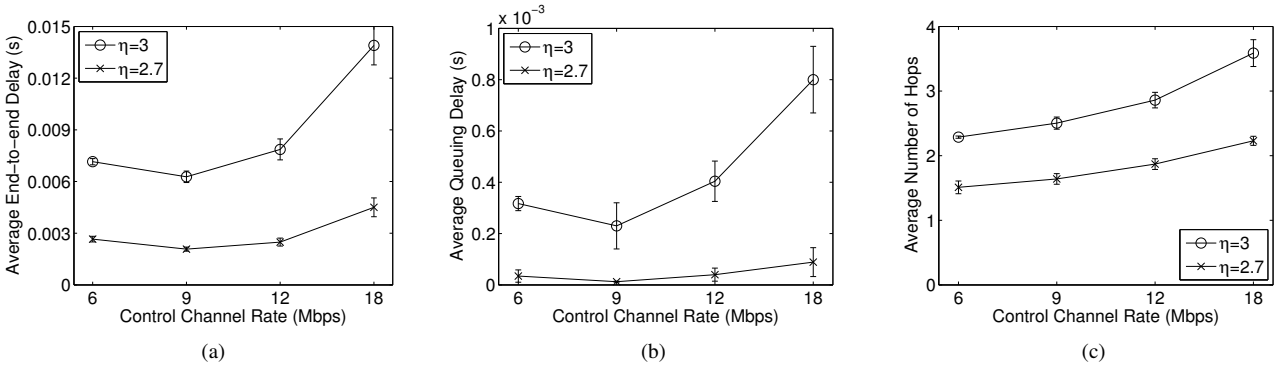

Figure 4. Average performance versus CCR for different path loss exponents (η), using $\lambda = 33.33$ packets/sec.

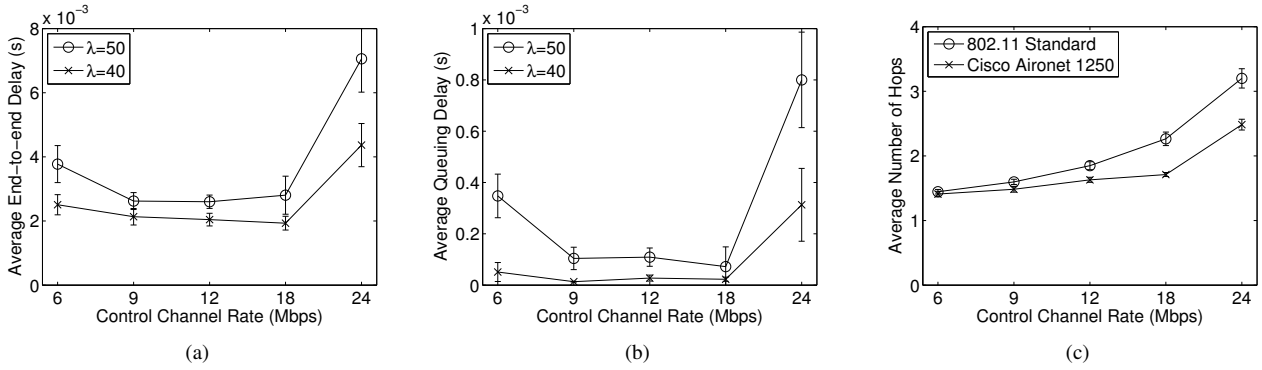

Figure 5. Average performance vs. CCR using the transmission rate/received power threshold table of the Cisco Aironet 1250 chipset.

Accordingly, the received power thresholds are -87, -86, -85, -84, -80, -78, -73, and -71 dBm for the transmission rates 6, 9, 12, 18, 24, 36, 48, and 54 Mbps, respectively. The optimal CCR is 12 Mbps when $\lambda = 50$ and 18 Mbps when $\lambda = 50$. In Fig. 5 (c), the number of hops increases more gradually in the case of the Cisco Aironet 1250 chipset than in the case of the 802.11 scheme. Hence, when the CCR is 12 or 18 Mbps, the decrease in link delay can offset the increase in the hop count.

VII. Conclusions

In this paper, we studied into the impact of the CCR on the MMAC performance in multi-hop networks, with the aim of determining the optimal CCR that minimizes the end-to-end delay. We used a $G/G/1$ queuing network to capture the delay components. Our analysis accounted for the various elements of generic CSMA/CA MMAC functionality, including exponential random backoff over the CC, control packet exchanges, and collisions. Our analysis was validated via NS-3 simulations. Further simulations

were conducted to assess the impact of various system parameters on the selection of the optimal CCR.

When the CCR is increased, the duration of control packet exchange is reduced so that CC overload can be reduced. However, increasing the CCR also increases the number of hops so that the number of transmissions to reach the destination is increased. As a consequence, the traffic intensity is increased and the collision likelihood is increased. Moreover, the increase in the hop count offsets the reduce in the duration of control packet exchange. When we use 802.11a parameters, results show that 9 Mbps is the optimal CCR instead of 6 Mbps which is the lowest one. Varying parameter values barely impacts the optimal CCR except the receive power threshold. The optimal CCR is increased to 18 Mbps when we use different receive power threshold values.

ACKNOWLEDGMENT

This work was made possible by NPRP grant no. NPRP 4-1034-2-385 from the Qatar National Research Fund (a member of Qatar Foundation). The statements made herein are solely the responsibility of the authors.

REFERENCES

[1] *Wireless LAN Medium Access Control (MAC) and Physical Layer (PHY) Specification*, IEEE Std. 802.11, Jun. 2007.

[2] A. Raniwala and T. Chiueh, "Architecture and algorithms for an IEEE 802.11-based multi-channel wireless mesh network," in *Proceedings of the 24th IEEE INFOCOM '05*, Mar. 13–17 2005, pp. 2223–2234.

[3] P. Bahl, R. Chandra, and J. Dunagan, "SSCH: slotted seeded channel hopping for capacity improvement in IEEE 802.11 adhoc wireless networks," in *Proceedings of the ACM MobiCom '04*, Sep. 26–Oct. 1 2004, pp. 216–230.

[4] K. Bian, J. Park, and R. Chen, "A quorum-based framework for establishing control channels in dynamic spectrum access networks," in *Proceedings of the 15th ACM MobiCom '09*, Sep. 20–25 2009, pp. 1051–1077.

[5] J. So and N. Vaidya, "Multi-channel MAC for ad hoc networks: handling multi-channel hidden terminals using a single transceiver," in *Proceedings of the ACM MobiCom '04*, May 24–26 2004, pp. 222–233.

[6] R. Maheshwari, H. Gupta, and S. Das, "Multichannel MAC protocols for wireless networks," in *Proceedings of the Third IEEE SECON '06*, Sep. 25–28 2006, pp. 393–401.

[7] N. Jain, S. Das, and A. Nasipuri, "A multichannel CSMA MAC protocol with receiver-based channel selection for multihop wireless networks," in *Proceedings of the 9th IEEE ICCCN '00*, Oct. 15–17, 2000, pp. 432–439.

[8] O. Incel, "A survey on multi-channel communication in wireless sensor networks," *Elsevier Computer Networks Journal*, vol. 10, no. 5, pp. 1389–1286, 2011.

[9] C. Cormio and K. Chowdhury, "A survey on MAC protocols for cognitive radio networks," *Elsevier Ad Hoc Networks Journal*, vol. 7, no. 7, pp. 1315–1329, 2009.

[10] T. Shu, S. Cui, and M. Krunz, "Medium access control for multi-channel parallel transmission in cognitive radio networks," in *Proceedings of the 49th IEEE GLOBECOM '06*, Nov. 27–Dec. 1 2006.

[11] F. Wang and M. Krunz, "Multi-channel spectrum-agile MAC protocol with adaptive load control," in *Proceedings of the 10th IEEE WoWMoM '09*, Jun. 15–19 2009.

[12] J. Mo, H. So, and J. Walrand, "Comparison of multichannel MAC protocols," *IEEE Trans. Mobile Comput.*, vol. 7, no. 1, pp. 50–65, Jan. 2008.

[13] J. Nieminen and R. Jantti, "Delay-throughput analysis of multi-channel MAC protocols in ad hoc networks," *EURASIP Journal on Wireless Communications and Networking*, vol. 2011, no. 108, Sep. 2011.

[14] L. Le, "Performance analysis of multi-channel MAC protocols in multi-hop ad hoc networks," in *Proceedings of the IEEE GLOBECOM '00*, Dec. 6–10, 2010.

[15] S. Cho, S. Ramasubramanian, O. Turkcu, and S. Subramaniam, "Performance analysis of multi-channel wireless infrastructure networks," in *Proceedings of the 17th IEEE LANMAN '10*, May 5–7, 2010.

[16] P. Kyasanur and N. H. Vaidya, "Capacity of multi-channel wireless networks: impact of number of channels and interfaces," in *Proceedings of the 11th ACM MobiCom '05*, Aug. 2005, pp. 43–57.

[17] D. Malone, K. Duffy, and D. Leith, "Modeling the 802.11 distributed coordination function in nonsaturated heterogeneous conditions," *IEEE/ACM Transactions on Networking*, vol. 15, no. 1, pp. 159–172, Feb. 2007.

[18] S. De, "On hop count and euclidean distance in greedy forwarding in wireless ad hoc networks," *IEEE Commun. Lett.*, vol. 9, no. 11, pp. 1000–1002, Nov. 2005.

[19] K. Chintalapudi and B. Radunovic, "WiFi-NC: WiFi over narrow channels," in *Proceedings of the USENIX NDSI '12 Conference*, Aug. 25-27 2012.

[20] T. Rappaport, *Wireless Communications: Principles and Practice*, 2nd ed. Upper Saddle River, NJ, USA: Prentice Hall PTR, 2001.

[21] G. Holland, N. Vaidya, and P. Bahl, "A rate-adaptive MAC protocol for multi-hop wireless networks," in *Proceedings of the ACM MobiCom '01*, 16–21, 2001.

[22] G. Bolch, S. Greiner, H. Meer, and K. Trivedi, *Queuing Networks and Markov Chains, chapter 10*. Newport Beach, CA: John Wiley and Sons Ltd., 1998.

[23] N. Bisnik and A. Abouzeid, "Queuing network models for delay analysis of multihop wireless ad hoc networks," in *Proceedings of the ACM IWCMC '06*, Jul. 3–6 2006, pp. 773–778.

[24] M. Carvalho and J. Garcia-Luna-Aceves, "Delay analysis of IEEE 802.11 in single-hop networks," in *Proceedings of the 11th IEEE ICNP '03*, Nov. 4–7 2003.

[25] S. Trivedi, *Probability and statistics with reliability, queuing, and computer science applications*, 2nd ed. Newport Beach, CA: John Wiley and Sons Ltd., 2002.

[26] A. Janssen and M. de Jong, "Analysis of contention tree algorithms," *IEEE Trans. Inf. Theory*, vol. 46, no. 6, Sep. 2000.

[27] Cisco, "Cisco aironet 1250 series access point," 2010. [Online]. Available: http://www.cisco.com/en/US/products/ps8382/index.html